

1 **Getting more out of FLAG-Tag co-immunoprecipitation mass spectrometry**
2 **experiments using FAIMS.**

3 **Ching-Seng Ang ^{*,1}, Joanna Sacharz ², Michael G. Leeming ¹, Shuai Nie ¹, Swati Varshney ¹, Nichollas E.**
4 **Scott ³ and Nicholas A. Williamson ^{*,1}**

5
6 ¹ Bio21 Mass Spectrometry and Proteomics Facility, The University of Melbourne, Parkville, Victoria 3052,
7 Australia

8
9 ² Department of Biochemistry and Molecular Biology, Bio21 Molecular Science and Biotechnology
10 Institute, University of Melbourne, Parkville, 3052 Victoria, Australia

11
12 ³ Department of Microbiology and Immunology, University of Melbourne at the Peter Doherty Institute
13 for Infection and Immunity, Melbourne 3000

14
15 *Correspondence to Ching-Seng Ang and Nichollas A. Williamson

16 Email: cang@unimelb.edu.au (ORCID ID: 0000-0001-7861-6719) and nawill@unimelb.edu.au (ORCID ID:
17 0000-0002-2173-3452)

18
19 Keywords: Co-IP mass spectrometry, FLAG Tag, FAIMS, ion mobility, Proteomics

20

21

22

23 **Abstract**

24 Co-immunoprecipitation of proteins coupled to mass spectrometry is critical for the understanding of
25 protein interaction networks. In instances where a suitable antibody is not available, it is common to graft
26 synthetic tags onto target protein sequences and allowing the use of commercially available antibodies
27 for affinity purification. A common approach is through FLAG-Tag co-immunoprecipitation. To allow the
28 selective elution of protein complexes, competitive displacement using a large molar excess of the tag
29 peptides is often carried out. Yet, this creates downstream challenges for the mass spectrometry analysis
30 due to the presence of large quantities of these peptides. Here, we demonstrate that Field Asymmetric
31 Ion Mobility Spectrometry (FAIMS), a gas phase ion separation device prior to mass spectrometry analysis
32 can be applied to FLAG-Tag co-immunoprecipitation experiment to increase the depth of protein
33 coverage. By excluding these abundant tag peptides, we were able to observe deeper coverage of
34 interacting proteins and as a result, deeper biological insights, without the need for additional sample
35 handling or altering sample preparation protocols.

36

37 **Introduction**

38 Many studies in systems biology focus on identifying and characterizing protein-protein interactions (PPI)
39 [1, 2]. Co-immunoprecipitation coupled with mass spectrometry (Co-IP/MS) is an extremely powerful
40 analytical technique and has been pivotal in PPI studies to identify protein complexes, co-factors and
41 signaling molecules [3, 4]. Over the last 20 years, Co-IP/MS approaches have evolved from multiple step
42 isolation procedures such as tandem affinity purification [5] to single step protocols [6] to improve the
43 sensitivity, robustness and ability to assess low affinity PPIs. Despite these improvements, the
44 fundamental approach has remained unchanged and are dependent on the use of specific antibodies
45 against a target protein which exists within a protein complex. Using these affinity reagents, immune
46 complexes are captured and interacting proteins identified using mass spectrometry. While there are
47 thousands of commercially available antibodies and with considerable research efforts being directed
48 toward cataloging these antibodies [7], not all affinity reagents are ideal for Co-IPs or are available for all
49 proteins.

50 To circumvent the need for protein specific reagents, a common strategy employed by researchers is to
51 tagged proteins with defined peptide or protein sequences. This involves coupling a small peptide or
52 protein tag to the N- or C-terminus of the target protein to minimize its effect on the protein function.
53 The tagged protein can then be detected using antibodies against the tag sequence rather than the target
54 protein itself. These tag-specific antibodies are available commercially and have been very well
55 characterized for their specificity and sensitivity. Examples of common protein tags include green
56 fluorescent protein (GFP), Glutathione S-Transferase (GST) and mCherry while FLAG, c-Myc, 6X-His and
57 Hemagglutinin (HA) are examples of recombinant peptide tags [8-11]. Proteins interacting with the tagged
58 target can be identified by eluting the interacting proteins from the target protein/antibody complex.
59 There are multiple sample preparation options for the elution step and one common approach is to elute
60 the complex from the affinity beads by using competitive displacement [9, 12] whereby molar excess of a

61 synthetic peptide (eg 2X Myc peptide; EQKLISEEDLEQKLISEEDL or 3X FLAG peptide;
62 MDYKDHDGDYKDHDIDYKDDDDK) is added to displace the bound proteins from the tag-specific antibody
63 under non-denaturation conditions. This approach limits the elution of non-specifically bound proteins
64 and allows the elution of complexes in buffers directly compatible with downstream digestion protocols.
65 Unfortunately, the presence of these excess peptides possesses an analytical challenge for subsequent
66 mass spectrometry analysis. Due to the high relative abundances, these 'contaminant' peptides rapidly
67 consume the ion storage capacity of ion trapping devices (C-trap, ion trap etc) [13, 14] and thus artificially
68 reduce the ability to detect other peptides (i.e. those arising from interactor proteins of interest) present
69 in the sample mix.

70 A range of techniques such as gas phased fractionation, BoxCar and Ion mobility (IM) based fractionation
71 [15-18] have been developed that aim to reduce the suppressive effects of highly abundant ions and to
72 increase proteome coverage. Ion mobility mass spectrometry is a technique whereby ions are separated
73 in the gas phase under influence of an electric field. Separation is related to a combination of their size,
74 shape and charge which influence the drift time - the time taken for the molecule to transverse towards
75 the detector [19, 20]. Multiple IM techniques have been developed that differ in the physical principles
76 utilized to achieve ion separation. IM systems can be broadly classified under linear and nonlinear
77 methods [21]. In the linear method, K_0 (reduced mobility) is assumed to be independent of the electric
78 field. These methods include Travelling Wave (TWIMS), Trapped Ion Mobility (TIMS), Drift Tube Ion
79 Mobility (DTIMS) and Differential Mobility Analyzers (DMA). In the nonlinear methods, K (mobility) of any
80 ion in any gas is dependent on the electric field. These methods include Differential Ion Mobility
81 Spectrometry (DIMS) and Field Asymmetric Ion Mobility (FAIMS). Each IM technique has its strengths and
82 are suitable for different applications. The IM systems can help address some of the issue of under
83 sampling due to the stochastic sampling of eluted peptides and bias caused by poor ion selection in a data
84 dependent acquisition methodology [22]. Multiple groups have utilized different forms of ion mobility

85 mass spectrometry to increase protein coverage in complex cellular systems [16, 18, 23]. We and others
86 have also used IM to enrich for modified peptides [24-26] or as a targeted SRM-like screening [27]
87 technique. These techniques took advantage of the unique collisional cross sectional properties of the
88 peptides on a linear IM device or by matching the applied compensation voltage of the targeted peptide
89 in a nonlinear FAIMS IM device.

90

91 FAIMS works by having two electrodes with alternating high and low electric field strength across these
92 electrodes. Separation of ions is by differences in their mobility in high and low electric fields [28, 29]. To
93 prevent collision of the ions with the electrode, the ions are diverted through application of a specific DC
94 compensation voltage (CV). The FAIMS device can therefore be used as a filtering device to remove
95 undesirable singly charged and interfering contaminating ions (eg solvent clusters). This allows the ion
96 current to be spread out and limit the proportion of high abundant species that contribute to the maximal
97 charge capacity of the C-trap [13]. The earlier version of the commercially available FAIMS device has met
98 with limited success due to significant ion losses [30]. Modifications to that FAIMS device by the Moritz
99 lab allowed them to be coupled to nanoLC-MS/MS systems, which significantly increased the depth of
100 proteome coverage in a complex yeast digest [31, 32]. The increased in coverage was attributed to the
101 reduction of singly charged chemical noise and resultant increase in the signal to noise of tryptic peptides.
102 More recent publications from the Coon and Thibaut labs using the second generation FAIMS device [16,
103 23] upon coupling them to Orbitrap Fusion Tribrid mass spectrometer show marked increase in protein
104 identification from whole cell lysate by ~10-55% than without FAIMS. Similar to the data shown by the
105 Moritz lab, singly charged species are almost constraint to a small CV range of between -10 and -40, are
106 being diverted and are instrumental in the increase in identification.

107

108 It is evident that FAIMS has the ability to increase proteome coverage in a highly complex sample by using
109 it as a prefiltering device to remove singly charged chemical noise. The benefit of FAIMS however is not
110 just limited to highly complex samples. In this manuscript, we were able to exploit the same prefiltering
111 principal in a FLAG-Tag Co-IP experiment to filter out highly abundant FLAG peptides that exists in multiple
112 charge states. These highly abundant FLAG peptides would otherwise interfere with the detection of the
113 less abundant peptides derived from the affinity target protein and its respective binding proteins. We
114 were able to demonstrate a huge improvement in terms of identified proteins in a supposedly 'simple'
115 Co-IP experiment and the resultant protein-protein interaction network analysis when compared to one
116 without application of FAIMS.

117

118 **Experimental Section**

119 **Affinity Enrichment of Flag-Tag proteins**

120 Affinity enrichment of FLAG-Tag protein experiment was performed from eHap knockout cells or HEK293
121 cells expressing FLAG-Tag protein as described previously [33]. Cell were solubilised in 1% (w/v) digitonin
122 in solubilization buffer (20mM Tris (pH 7.4), 50mM NaCl, 10% (v/v) Glycerol, 0.1 mM EDTA, 5U benzonase
123 (Merck Millipore), 2mM MgCl₂). Following clarification of cell lysate by centrifugation (20,000g, 10 mins,
124 4°C), 500 µg protein was added to spin columns (Pierce) containing anti-FLAG M2 affinity resin (Merck)
125 and allowed to incubate rotating for two hours at 4°C. Non-specifically bound proteins were then removed
126 by washing with 20x column volumes of ice-cold solubilization buffer containing 0.1% (w/v) digitonin.
127 Proteins were eluted with 50 µl of 100 µg/mL of 3X FLAG tag peptide (Merck) in solubilization buffer
128 followed by acetone precipitation (overnight, -20°C). Proteins were then pelleted by centrifugation
129 (21,000g, 10 mins, 4°C), washed with ice-cold acetone and air-dried. The pellet was then resolubilised by
130 sonification in with 8M urea in 50 mM ammonium bicarbonate (ABC). Samples were reduced and

131 alkylated with 50mM TCEP (ThermoFisher) and 500 mM Chloroacetamide (Merck) (30mins, 37°C,
132 shaking). Elutions were diluted to 2M urea in 50mM ABC and digested in trypsin (Promega) overnight at
133 37°C. The digest was acidified to a final concentration of 1% (v/v) trifluoroacetic acid (TFA) and peptides
134 were desalted with stagetips containing 2x plugs of 3M™ Empore™ SDB-XC substrate (SUPELCO). Stagetips
135 were activated with 100% Acetonitrile (ACN) and washed with 0.1% (v/v) TFA, 2% (v/v) ACN prior to
136 binding of peptides. Samples were eluted in 80% ACN, 0.1% TFA and dried completely in a SpeedVac.
137 Peptides were reconstituted in 2% ACN, 0.1% TFA and transferred to autosampler vials for analysis by LC
138 MS/MS

139 **LC MS/MS analysis**

140 LC MS/MS was carried out using the Fusion Lumos Orbitrap mass spectrometers with the FAIMS Pro
141 interface (Thermo Fisher, USA) and as described previously [26]. The LC system was equipped with an
142 Acclaim Pepmap nano-trap column (Dionex-C18, 100 Å, 75 µm x 2 cm) and an Acclaim Pepmap RSLC
143 analytical column (Dionex-C18, 100 Å, 75 µm x 50 cm). Tryptic peptides were injected into the enrichment
144 column at an isocratic flow of 5 µL/min of 2% (v/v) acetonitrile containing 0.1% (v/v) formic acid for 6 min,
145 applied before the enrichment column was switched in-line with the analytical column. The eluents were
146 0.1% (v/v) formic acid (solvent A) in water and 100% (v/v) acetonitrile in 0.1% (v/v) formic acid (solvent
147 B). The flow gradient was (i) 0-6 min at 3% B; (ii) 6-35 min, 3-22% B; (iii) 35-40 min, 22-40% B; (iv) 45-50
148 min, 40-80% B; (v) 50-55 min, 80-80% B; (vi) 55-56 min 85-3% and equilibrated at 3% B for 10 min before
149 injecting the next sample. Tune version 3.3.2782.32 was used. For non-FAIMS experiments, the mass
150 spectrometer was operated in the data-dependent acquisition mode, whereby full MS1 spectra were
151 acquired in a positive mode at 60000 resolution. The 'top speed' acquisition mode with 3 s cycle time on
152 the most intense precursor ion was used, whereby ions with charge states of 2 to 7 were selected.
153 Automated gain control (AGC) target was set to standard with auto maximum injection mode. MS/MS
154 analyses were performed by 1.6 *m/z* isolation with the quadrupole, fragmented by CID with collision

155 energy of 35 %, activation time of 10 ms and activation Q of 0.25. Analysis of fragment ions was carried
156 out in the ion trap using the 'Turbo' speed scanning mode. Dynamic exclusion was activated for 30 s. For
157 FAIMS-enabled experiments, the mass spectrometer was operated in the data-dependent acquisition
158 mode scanning from m/z 300-1600 at 60000 resolution. FAIMS separations were performed with the
159 following settings: inner electrode temperature = 100 °C, outer electrode temperature = 100 °C, FAIMS
160 carrier gas flow = 0 L/min. The FAIMS carrier gas was N₂. Cycle time using the 'top speed acquisition' mode
161 for single CV experiment were 3 s and, for experiments wherein two CVs (-40 and -60) were applied and
162 cycle time was 1.5 s each. MS/MS analyses were performed by 1.6 m/z isolation with the quadrupole,
163 fragmented by CID with collision energy of 35 %, activation time of 10 ms and activation Q of 0.25. Analysis
164 of fragment ions was carried out in the ion trap using the 'Turbo' speed scanning mode. Dynamic exclusion
165 was activated for 30 s.

166

167 For LC MS/MS experiments on an Orbitrap Eclipse the nanoLC conditions were kept constant. The mass
168 spectrometer was operated in the data-dependent acquisition mode, whereby full MS1 spectra were
169 acquired in a positive mode at 60000 resolution. Tune version was 3.3.2782.34. The 'top speed' acquisition
170 mode with 3 s cycle time on the most intense precursor ion was used, whereby ions with charge states of
171 2 to 7 were selected. AGC target was set to standard with auto maximum injection mode. MS/MS analyses
172 were performed by 1.6 m/z isolation with the quadrupole, fragmented by CID with collision energy of 35
173 %, activation time of 35 ms and activation Q of 10. Analysis of fragment ions was carried out in the ion
174 trap using the 'Turbo' speed scanning mode. Dynamic exclusion was activated for 30 s.

175 For LC MS/MS experiments on an Orbitrap Exploris 480, the nanoLC conditions were kept constant. The
176 mass spectrometer was operated in the data-dependent acquisition mode, whereby full MS1 spectra
177 were acquired in a positive mode at 60000 resolution. Tune version was 2.0.182.25. The 'top speed'

178 acquisition mode with 3 s cycle time on the most intense precursor ion was used, whereby ions with
179 charge states of 2 to 7 were selected. MS/MS analyses were performed by 1.6 m/z isolation with the
180 quadrupole, fragmented by HCD with collision energy of 30%. MS2 resolution was at 15000 Dynamic
181 exclusion was activated for 30 s. AGC target was set to standard with auto maximum injection mode.
182 Dynamic exclusion was activated for 30 s.

183

184 **Database search**

185 Database searches was carried out using Proteome Discoverer (v2.4) with the SequestHT search engine
186 or the Maxquant proteomics software package (version 2.0.1.0) against a *Homo Sapiens* database
187 (SwissProt Taxonomy ID 9606, updated Feb 2021). The SequestHT search parameters are Trypsin as the
188 cleavage enzyme and a maximum of 2 missed cleavages. Precursor and fragment mass tolerances of 10
189 ppm and 0.6 Da, respectively. The default instrument specific search parameters were used in the
190 Maxquant specific searches. For both search engines, carbamidomethyl cysteine was set as fixed
191 modification, and oxidation of methionine and acetylation of the protein N-terminus were considered as
192 variable modifications. Protein and peptides groups were set to a maximum false discovery rate (FDR) of
193 < 0.01 as determined by the Percolator or Maxquant algorithm [34, 35]. Peak area determination was
194 carried out using the Skyline software [36]. Statistical analysis was carried out using the Perseus
195 computational platform [37]. To correct for multiple-hypothesis testing, significant hits are defined using
196 Student's T-test, truncated by permutation-based FDR threshold of 0.05 (250 randomization) and S0
197 factor of 2.0 [38]. Protein-protein interaction network and functional enrichment analysis was performed
198 using STRING [39].

199

200 **Results**

201 The total ion chromatogram (TIC) of a FLAG Co-IP/MS experiment following competitive displacement
202 with 3X FLAG peptide and *in solution* digest is shown in Figure 1A. Three dominant peaks are visible in the
203 chromatogram between 16.0 min and 26 min. The later TIC peak is being dominated by few highly charged
204 ions, corresponding to multiply charged species of the 3X FLAG peptide - MDYKDHDGDYKDHDIDYKDDDDK
205 (2+, 3+, 4+, 5+ and 6+). The earlier TIC peaks consist of a number of modified or truncated versions of the
206 3X FLAG peptide e.g. oxidized methionine, trypsin cleavage products (MDYYK↓DHDGDYKDHDIDYKDDDDK)
207 and the oxidized forms of these tryptic peptides. These high abundant peptides typically co-elute with
208 other tryptic peptides within the 10 min elution window. This result is representative of a large fraction
209 of Co-IP/MS experiments wherein the most abundant ions detected are introduced as byproducts of the
210 assay itself and do not correspond to peptides arising from interactor proteins.

211

212 The most abundant ions observed in each of these major chromatographic peaks correspond to highly
213 charged (+4 to +6) 3X FLAG-derived peptide ions (Figures 1B and 1C). Given that tryptic peptides produced
214 from analyte proteins are most commonly observed in +2 or +3 charge states, the higher charges of the
215 3X FLAG contaminant ions offered the possibility that these could be removed in the gas phase via FAIMS.
216 The synthetic 3X FLAG peptide was first analyzed on the FAIMS/Lumos Orbitrap mass spectrometer with
217 incrementally increasing compensation voltages from CV-20 to CV-70 in steps of 10 (Figure 2). With the
218 exception of the $[M+4H]^{4+}$ precursor at CV-60 and CV-70, all the other charge states of the 3X FLAG were
219 reduced in measured intensity between 30% and 100% (Figure 2, Supplementary Table 1). Next, a FLAG
220 Co-IP experiment was carried out on a whole cell lysate. Following *in solution* digest, the same sample was
221 repeatedly analyzed using the FAIMS/Lumos Orbitrap with the same incrementally increasing
222 compensation voltages to assess the number of proteins, peptides, and peptide spectral matches (PSM)
223 identified under these varying FAIMS conditions. Without FAIMS, 365 proteins, 1362 peptides and 1603
224 PSM were identified (at 1% FDR). The greatest improvement in identifications were when FAIMS was

225 operated with a CV of -40. This led to gains of 93%, 58% and 51% in proteins, peptides and PSM,
226 respectively, as compared to analysis of the same sample without FAIMS (Figure 3A). The remainder of
227 the single CVs tested led to either comparable (CV- 30 and -50) or substantially lower (CV -20, -60, -70)
228 proteins, peptides and PSM upon database searching.

229
230 While the greatest improvement in protein identifications was observed for CV-40, it is well documented
231 that different, and perhaps complementary, subsets of peptides may be preferentially detected at
232 alternative CVs or internal CV stepping [23]. To assess whether identification numbers may be improved
233 by employing internal CV stepping, the same FLAG Co-IP digest was re-analyzed with two internal CV steps
234 of -40 and -60. Here, 734 proteins, 2550 peptides and 2904 PSMs were identified following database
235 searching. This translates to a 100%, 59% and 81% gain as compared to without FAIMS. This is almost a 2-
236 fold increase in the total protein identification but critically, the number of proteins that was exclusively
237 identified in the FAIMS experiment was 409 when two internal CV stepping were applied as compared to
238 only 40 without FAIMS (Figure 3D). The distribution of the different charge species selected for MS/MS
239 follows a trend of decreasing 2+ peptides and increasing 4+ and 5+ peptides with more negative CVs
240 (Figure 3E). 3+ peptides appear to be uniformly distributed and within ~20%-45% of all measured MS1
241 features across CV-30 to CV-70. We repeated this experiment on an independent FLAG Co-IP experiment
242 targeting a different FLAG-Tag protein, and observed similar and large increase in the protein, peptide
243 and PSM (Supplementary Figure 1).

244
245 The TIC and number of PSM identifications were plotted across the HPLC retention time at the regions
246 (16-26min) corresponding to the elution time of the 3X FLAG peptides (Figure 1). With FAIMS rapidly
247 switching between CVs of -40 and -60 FAIMS, there is a noticeable drop in the MS1 ion injection time and

248 a corresponding increase in the identified PSM (Figure 4B and 4C). At those alternating CV values, the 5+,
249 6+ charged species and also a large percentage of the 4+ charged species can be effectively reduced or
250 removed (Figure 2), which otherwise would have contributed to filling up a portion of the limited charge
251 capacity of the C-trap. The total number of identified PSM between the 16-26 minute elution window at
252 CV-40 and CV-60 is 374 and 115, respectively. Without FAIMS, the total number of identified PSM is only
253 120.

254

255 To determine if sample complexity has a large effect on protein and peptide identification on the Orbitrap
256 Lumos, a commercial HeLa tryptic digest (100ng on column) was analyzed using two internal CV stepping
257 (-40 and -60) and without FAIMS. With FAIMS, 37% and 23% more proteins and peptides, respectively,
258 were identified as compared to without FAIMS. To determine if the increase in identification is not due to
259 the analytical mass spectrometer, the FLAG Co-IP digest was analyzed on the next generation Orbitrap
260 Eclipse and Orbitrap Exploris 480 mass spectrometer using similar LC-MS/MS conditions. The results were
261 then compared with the same FLAG Co-IP digest analyzed on the FAIMS/Lumos Orbitrap with two CV
262 internal stepping (-40 and -60). With FAIMS/Lumos Orbitrap, 70.7% and 114.9% more proteins were
263 identified compared to Eclipse and Exploris 480, respectively. On the peptide level, there were 43.3% and
264 81.1% more from FAIMS/Lumos compared to Eclipse and Exploris 480, respectively (Supplementary Table
265 2).

266

267 All the above Co-IP experiment were carried using the same *in solution* digested sample and comparing
268 protein and peptide identifications, with and without FAIMS. We sought to see if the improvement were
269 indeed biologically relevant in a comparative Co-IP experiment. For this, a FLAG-Tag transmembrane
270 protein was used for immunoprecipitation of proteins after treatment with a drug that targets the

271 membrane ion channel. All experiment were performed in triplicates and the *in solution* digested samples
272 were analyzed on the Lumos Orbitrap mass spectrometer with and without FAIMS. After subtracting
273 proteins identified from the negative controls, statistical analysis was carried out to highlight proteins that
274 were significantly changed in abundances upon drug treatment (Figures 5A and 5B). These significantly
275 changed proteins were combined with proteins that are identified exclusively from the drug treatment
276 group (identified in all 3 replicates in drug treatment and absent in all the non-treatment replicates). From
277 the above selection criteria, a list of 265 proteins with FAIMS and 117 proteins without FAIMS was
278 generated (Supplementary Table 3). Protein-protein interaction network and functional enrichment
279 analysis was then carried using STRING (Figures 5D and 5E). We applied the highest confidence score
280 (0.900) and display only edges from where proteins are part of a physical complex (STRING physical
281 subnetworks feature). From these, a highly significant protein-protein interaction (PPI) enrichment for
282 both Co-IP with FAIMS (PPI enrichment p value $<1.0e-16$) and without FAIMS (PPI enrichment p value =
283 $1.3e-11$) was obtained. For clarity, the disconnected nodes in the network were not displayed. There are
284 a total of 51 protein (86 edges) enriched from known physical complexes with FAIMS versus 18 proteins
285 (17 edges) from without FAIMS. The top 2 molecular function enrichment from both FAIMS and without
286 FAIMS were related to SNAP receptor (red bubble) and SNARE binding (blue bubble). The endomembrane
287 system (green bubble) was the topmost enriched subcellular localization for both FAIMS and without
288 FAIMS Co-IP experiment.

289

290 **Discussion**

291 Given that FLAG-Tag Co-IP experiments typically produce large molar excesses of contaminant peptides
292 derived from peptides used in competitive displacement, we reasoned that deeper profiling of interacting
293 species could be achieved by developing methods to reduce the suppressive effects of high-abundance

294 ions on mass spectrometric detection of low-abundance species. We have utilized FAIMS as a gas phase
295 filtering technique, to filter or reduce the highly abundant synthetic 3X FLAG peptides in a FLAG Co-IP
296 mass spectrometry experiment and have increased the depth of proteome coverage. The total numbers
297 of proteins identified from FLAG-Tag Co-IPs increased two-fold when FAIMS filtering was employed with
298 two, rapid compensation voltage steps (-40 and -60) compared to analyses of the same sample when
299 FAIMS was not used. Critically, a much larger number of proteins were exclusively identified with the
300 application of the optimal FAIMS-filtering method versus when no FAIMS is used.

301

302 It should be noted that a range of techniques are currently available to reduce interference from high-
303 abundance peptides. For example, the excess FLAG peptides could be removed with an offline cleanup
304 process or by running it off an SDS PAGE gel, size exclusion columns, molecular weight filtration etc. The
305 downside is that it requires additional offline sample handling steps and will likely introduce experimental
306 variabilities. A single LC MS/MS experiment with increased depth is still the preferred methodology in a
307 Co-IP/MS experiment. In contrast to these existing methods, the FAIMS methodology presented here does
308 not require any additional sample handling steps, fractionation or library construction and is completely
309 amenable to standard, single-shot data-dependent acquisition.

310

311 We reasoned that one of the largest contributing factors to the increased protein identification is that
312 FAIMS can divert singly charged chemical noise, resulting in increased signal to noise as also demonstrated
313 in earlier studies [16, 23, 31, 32]. Not allowing a few abundant peptides, such as the synthetic 3X FLAG
314 peptide fill up the limited charge capacity of the ion storage device is another significant contributing
315 factor. The later phenomenon has been exploited to increase the proteome coverage in other gas phase
316 fractionation strategies [15, 17, 40]. For example, in the more recent BoxCar acquisition strategy [17], ion

317 injection is limited to a portion of the total mass range so as to distribute the maximal charge capacity.
318 This is to limit the proportion of highly abundant or well ionizing peptides affecting ion accumulation in
319 the C-traps, which typically can be filled up in less than 1ms [13]. One millisecond is typically less than 1%
320 of the transient time required to generate a high-resolution mass spectrum in the Orbitrap, which takes
321 between 128-256ms (resolution dependent). What that means is >99% of these ions are not being used
322 for mass analysis. When scanning in limited mass ranges, these gas phased fractionation methodologies
323 can spread out the abundant species which otherwise rapidly fill up the C-trap, thus allowing increased
324 filling time for the less abundant peptides. Although the MS1 overhead and duty is increased with multiple
325 m/z windows, the overall benefits in terms of increased identification of low-level peptides is substantial
326 with up to a 10-fold gain in dynamic range [17]. In a FLAG Co-IP experiment, the presence of the high
327 abundant synthetic 3X FLAG peptide will rapidly fill up the C-trap and can affect accumulation of other
328 low abundant peptides. We have empirically determined the relationship between the applied CV and the
329 charged characteristic for the 3X FLAG peptide (Figure 2). By applying different FAIMS CVs, gas phased
330 fractionation can be used to filter out the high abundant 3X FLAG peptides at different charge states. The
331 charge distribution and mass to charge ratio (m/z) of precursor peptides across multiple CVs in a complex
332 Hela and yeast digest have previously been reported [23, 31, 32]. In addition to the charge states,
333 precursor mass to charge ratio (m/z) also have a large impact on the FAIMS mobility. Optimal
334 compensation field (E_c) for multiply charged peptides varies and the largest m/z are generally observed
335 over lower magnitude E_c and smaller m/z generally over higher E_c and are charge state dependent [32].
336 The reported Co-IP data is in general agreement with the complex digest reported in the earlier
337 investigations, with doubly charged precursors found predominantly at the lower CV, triple charged
338 precursors distributed over a wider CV and higher charge densities observed for more negative CVs.
339

340 When performing that as a single LC-MS/MS experiment and two internal CV stepping, a large proportion
341 of the intense 4+, 5+ and 6+ FLAG peptide is filtered at the CV-40 step. This allows gas phase enrichment
342 of the lower charged state peptides derived from the affinity target protein and its respective binding
343 proteins. When switching to the CV-60 step, the characteristics of the peptides differs, allowing
344 identification of a different set of peptides. This is also evident by the decreased MS1 TIC and
345 corresponding increased PSM during the 16-26 minute elution window of the synthetic 3X FLAG peptide
346 (Figure 4). In contrast to the BoxCar acquisition strategy, the minimal increased in MS1 overhead in a
347 FAIMS type experiment has lower impact on the overall instrument duty cycle as only 2 internal CV
348 stepping are used, and the complexity of Co-IP experiment is generally not high.

349

350 We sought to establish if the large increase in protein and peptide identifications is a phenomenon that
351 is augmented in Co-IP experiment and not due to sample complexity or instrumentation. To do that, the
352 differences in identifications using a highly complex whole cell digest with and without FAIMS was carried
353 out. In a complex whole cell digest and using FAIMS, there were 37% and 23% more proteins and peptides
354 identified, respectively, than without FAIMS (Supplementary Table 2). This is in general agreement with
355 the work published by the Coon lab [23] where they showed FAIMS (different CVs compared to this
356 manuscript) providing similar increase in protein identification with the same 60 min analysis time. In the
357 FAIMS Flag-Tag Co-IP experiment, where sample complexity is much lower, there is a 100% and 59%
358 increase in proteins and peptides, respectively. This suggests, removal of singly charged chemical noise
359 and high abundant contaminant 3X FLAG peptides can have a more profound effect in samples of lesser
360 complexity. The same Co-IP experiment was then analyzed without FAIMS on the Orbitrap Lumos and 2
361 newer Orbitraps (Orbitrap Eclipse and Exploris 480) to determine if the same increase in protein and
362 peptide identifications can be achieved with newer instrumentation. The number of identified proteins,
363 peptides and PSM was similar between Orbitrap Eclipse and Lumos and Exploris 480 having the least

364 number of identifications (supplementary Table 2). Again, when comparing all 3 experiments with
365 FAIMS/Lumos, protein, peptide and PSM identification are much higher when FAIMS was used. The
366 Orbitrap Eclipse and Exploris 480 are to date, the latest generation Orbitrap mass spectrometer with
367 improvement in the quad filter, FTMS overheads and better ion transmission [41, 42]. These newer
368 generation of Orbitrap mass spectrometers have been shown to increase the identification rates of
369 proteins as compared to the Fusion Lumos Orbitrap by up to 20% in a complex Hela digest or single cell
370 proteome study where sensitivity is of utmost importance [41, 43]. The much higher protein and peptide
371 identifications clearly shows the increase identification on FAIMS/Lumos cannot be replicated with newer
372 instrumentation. The FAIMS device can provide increased depth in a highly complex sample but for a
373 relatively low complexity sample like a Co-IP experiment, the improvement afforded by filtering out the
374 dominating ion species is much greater.

375 Lastly, we look into the STRING protein-protein interaction networks generated from identified proteins
376 with and without FAIMS. It quickly became apparent that the network generated from the FAIMS dataset
377 is denser, more informative and has more proteins identified than without FAIMS (Figure 5C). Whilst not
378 focusing on any biological interpretation, we sought to find out what gains were achieved. Instead of
379 presenting indirect (functional) interactions where the PPI network can become overly dense and with
380 boundless overlapping nodes, these networks are reported as a more conservative physical subnetwork.
381 This allow us to look at proteins that are experimentally shown to be physically linked and without the
382 added complications of functional interactions derived from computational means [44]. For added clarity,
383 disconnected nodes are also removed from the analysis. With FAIMS, there are 51 proteins that are
384 connected through direct physical interactions versus 17 without FAIMS. The vast majority of these
385 proteins are associated with the endomembrane system, which correlates well with the bait protein being
386 a transmembrane protein. The top 2 enriched molecular function from the FAIMS and no FAIMS dataset
387 are similar and are related to SNARE binding and SNAP receptor activity. SNARE (or SNAP REceptor)

388 proteins are made up of a large protein superfamily of more than 60 members in mammalian cells and
389 are involved in membrane fusion along the secretory and endomembrane systems [45]. Although analysis
390 without FAIMS showed similar enrichment in molecular functions, more proteins from the SNARE
391 complexes such as Syntaxins (STX), STXBP, VTI1B, VAMP, SNAP, SEC22A, GOSR2 and RAB [46] are enriched
392 with FAIMS. These SNARE proteins are on top of many more interacting proteins, especially those
393 associated with the endomembrane systems (Figure 4D, green bubble). Being able to identify different
394 STX proteins can provide us with additional information on the cellular localization of these complexes.
395 For example, different members of the SNARE proteins are distributed in distinct subcellular localization,
396 which form specific SNARE complexes to mediate different transport events [46]. 9 different STX proteins
397 versus 3 STX proteins were identified from FAIMS and without FAIMS, respectively. STX5 is present in at
398 least three different SNAREpins, regulating Golgi trafficking and is thought to be the master SNARE of the
399 Golgi apparatus [47]. STX6 and STX16 form one of two Golgi SNAREpins with VTI1A and VAMP4 [48].
400 Consolidating the above information allow us to speculate an enhanced interaction of the Golgi network
401 with the transmembrane protein, upon treatment with the membrane ion channel drug. That cannot be
402 said with the Co-IP experiment analyzed without FAIMS. We cannot discount there are also proteins that
403 are uniquely identified from the without FAIMS experiment, but the large increase in protein identification
404 and resultant denser PPI network represents the extension of the depth of proteome coverage, potentially
405 revealing previously unknown protein partners and in our view should be the method of choice for such
406 experiment.

407 Discovery and functional characterization of protein-protein interaction network is challenging. This
408 requires sound experimental planning, the right bait protein(s), high yield of bait proteins and in-depth
409 identification of the interacting proteins. While a full biological analysis of these entities is beyond the
410 scope of this manuscript, these proteins differentially detected with FAIMS could potentially be missing
411 links in protein complexes or low level transient interactors etc. While FAIMS enabled methodology has

412 already been documented to increase proteome coverage for complex proteomics samples we show here
413 that it can have a proportionately greater impact on “simple” or low complexity samples.

414

415 **Data Availability**

416 The mass spectrometry proteomics data have been deposited to the ProteomeXchange Consortium via
417 the PRIDE partner repository with the dataset identifier PXD028965

418

419 **Author Contributions**

420 CSA and NAW designed the research, CSA developed methodology, CSA, MGL, SN, SV performed
421 experiments, all authors analyzed data and wrote the paper.

422

423 **Supporting information**

424 Supplementary data to this article can be found online at ...

425

426 **Supplementary Figure 1:** Analyzing the protein and peptide identification from a second independent
427 FLAG Co-IP experiment.

428 **Supplementary Table 1:** Comparing intensities of the different charge states of the 3X FLAG peptide across
429 different CVs.

430

431 **Supplementary Table 2:** Comparing the identification rate across 3 different Orbitrap Mass Spectrometers

432

433 Supplementary Table 3: List of significantly changed proteins used for STRING analysis

434

435 **References**

436

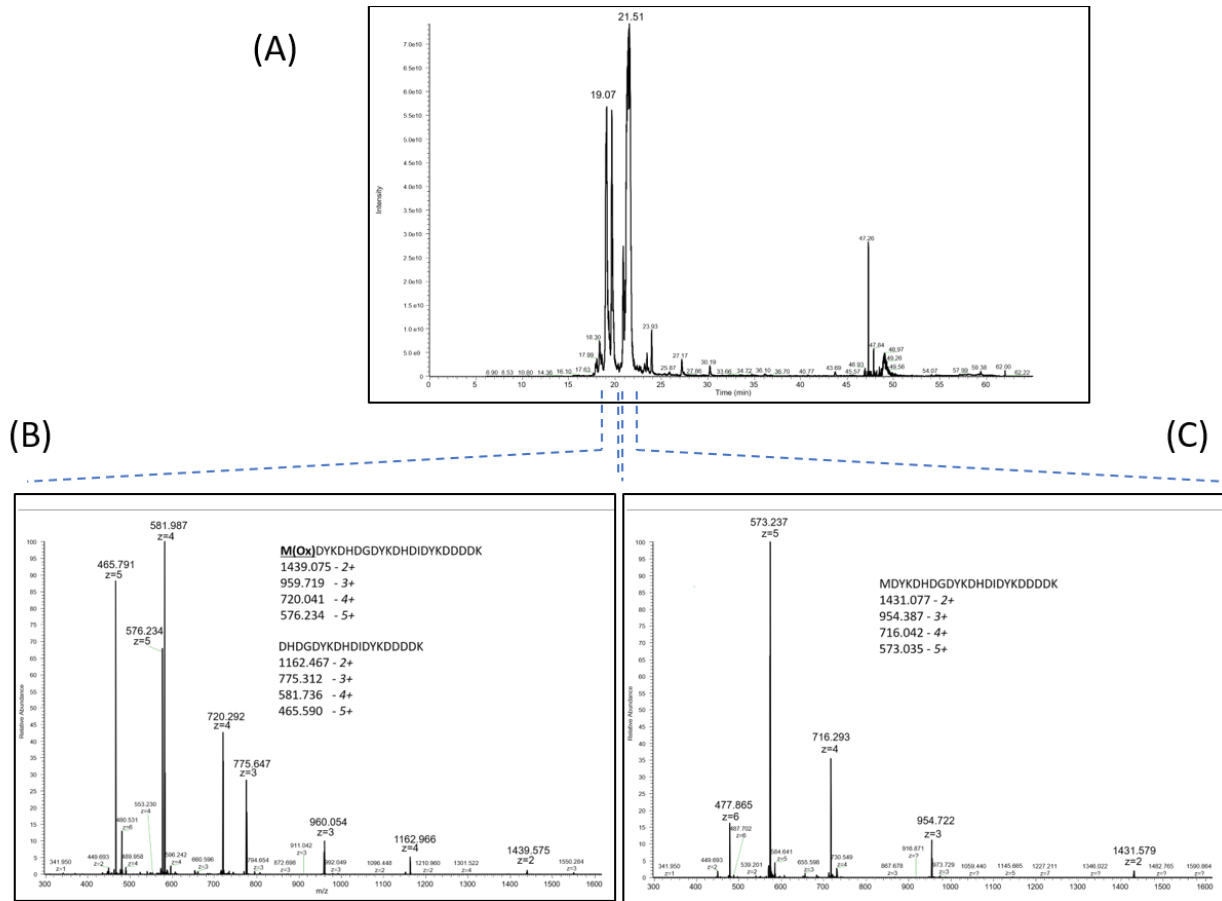
- 437 [1] T. Rolland, M. Tasan, B. Charlotheaux, S.J. Pevzner, Q. Zhong, N. Sahni, S. Yi, I. Lemmens, C. Fontanillo,
438 R. Mosca, A. Kamburov, S.D. Ghiassian, X. Yang, L. Ghamsari, D. Balcha, B.E. Begg, P. Braun, M. Brehme,
439 M.P. Broly, A.R. Carvunis, D. Convery-Zupan, R. Corominas, J. Coulombe-Huntington, E. Dann, M. Dreze,
440 A. Dricot, C. Fan, E. Franzosa, F. Gebreab, B.J. Gutierrez, M.F. Hardy, M. Jin, S. Kang, R. Kiros, G.N. Lin, K.
441 Luck, A. MacWilliams, J. Menche, R.R. Murray, A. Palagi, M.M. Poulin, X. Rambout, J. Rasla, P. Reichert,
442 V. Romero, E. Ruysinck, J.M. Sahalie, A. Scholz, A.A. Shah, A. Sharma, Y. Shen, K. Spirohn, S. Tam, A.O.
443 Tejada, S.A. Trigg, J.C. Twizere, K. Vega, J. Walsh, M.E. Cusick, Y. Xia, A.L. Barabasi, L.M. Iakoucheva, P.
444 Aloy, J. De Las Rivas, J. Tavernier, M.A. Calderwood, D.E. Hill, T. Hao, F.P. Roth, M. Vidal, A proteome-
445 scale map of the human interactome network, *Cell* 159(5) (2014) 1212-1226.
- 446 [2] P.C. Havugimana, G.T. Hart, T. Nepusz, H. Yang, A.L. Turinsky, Z. Li, P.I. Wang, D.R. Boutz, V. Fong, S.
447 Phanse, M. Babu, S.A. Craig, P. Hu, C. Wan, J. Vlasblom, V.U. Dar, A. Bezginov, G.W. Clark, G.C. Wu, S.J.
448 Wodak, E.R. Tillier, A. Paccanaro, E.M. Marcotte, A. Emili, A census of human soluble protein complexes,
449 *Cell* 150(5) (2012) 1068-81.
- 450 [3] R.B. Free, L.A. Hazelwood, D.R. Sibley, Identifying novel protein-protein interactions using co-
451 immunoprecipitation and mass spectroscopy, *Curr Protoc Neurosci Chapter 5* (2009) Unit 5 28.
- 452 [4] K. Markham, Y. Bai, G. Schmitt-Ulms, Co-immunoprecipitations revisited: an update on experimental
453 concepts and their implementation for sensitive interactome investigations of endogenous proteins,
454 *Anal Bioanal Chem* 389(2) (2007) 461-73.
- 455 [5] G. Rigaut, A. Shevchenko, B. Rutz, M. Wilm, M. Mann, B. Seraphin, A generic protein purification
456 method for protein complex characterization and proteome exploration, *Nat Biotechnol* 17(10) (1999)
457 1030-2.
- 458 [6] E.C. Keilhauer, M.Y. Hein, M. Mann, Accurate protein complex retrieval by affinity enrichment mass
459 spectrometry (AE-MS) rather than affinity purification mass spectrometry (AP-MS), *Mol Cell Proteomics*
460 14(1) (2015) 120-35.
- 461 [7] M. Uhlen, L. Fagerberg, B.M. Hallstrom, C. Lindskog, P. Oksvold, A. Mardinoglu, A. Sivertsson, C.
462 Kampf, E. Sjostedt, A. Asplund, I. Olsson, K. Edlund, E. Lundberg, S. Navani, C.A. Szigartyo, J. Odeberg, D.
463 Djureinovic, J.O. Takanen, S. Hober, T. Alm, P.H. Edqvist, H. Berling, H. Tegel, J. Mulder, J. Rockberg, P.
464 Nilsson, J.M. Schwenk, M. Hamsten, K. von Feilitzen, M. Forsberg, L. Persson, F. Johansson, M. Zwahlen,
465 G. von Heijne, J. Nielsen, F. Ponten, Proteomics. Tissue-based map of the human proteome, *Science*
466 347(6220) (2015) 1260419.
- 467 [8] S. Munro, H.R. Pelham, Use of peptide tagging to detect proteins expressed from cloned genes:
468 deletion mapping functional domains of *Drosophila* hsp 70, *EMBO J* 3(13) (1984) 3087-93.
- 469 [9] R. Hernan, K. Heuermann, B. Brizzard, Multiple epitope tagging of expressed proteins for enhanced
470 detection, *Biotechniques* 28(4) (2000) 789-93.
- 471 [10] J. DeCaprio, T.O. Kohl, Tandem Immunoaffinity Purification Using Anti-FLAG and Anti-HA Antibodies,
472 *Cold Spring Harb Protoc* 2019(2) (2019).
- 473 [11] A. Louche, S.P. Salcedo, S. Bigot, Protein-Protein Interactions: Pull-Down Assays, *Methods Mol Biol*
474 1615 (2017) 247-255.
- 475 [12] H.R. Hoogenboom, A.D. Griffiths, K.S. Johnson, D.J. Chiswell, P. Hudson, G. Winter, Multi-subunit
476 proteins on the surface of filamentous phage: methodologies for displaying antibody (Fab) heavy and
477 light chains, *Nucleic Acids Res* 19(15) (1991) 4133-7.

- 478 [13] R.A. Zubarev, A. Makarov, Orbitrap mass spectrometry, *Anal Chem* 85(11) (2013) 5288-96.
- 479 [14] D.J. Douglas, A.J. Frank, D. Mao, Linear ion traps in mass spectrometry, *Mass Spectrom Rev* 24(1)
- 480 (2005) 1-29.
- 481 [15] E.C. Yi, M. Marelli, H. Lee, S.O. Purvine, R. Aebersold, J.D. Aitchison, D.R. Goodlett, Approaching
- 482 complete peroxisome characterization by gas-phase fractionation, *Electrophoresis* 23(18) (2002) 3205-
- 483 16.
- 484 [16] S. Pfammatter, E. Bonneil, F.P. McManus, S. Prasad, D.J. Bailey, M. Belford, J.J. Dunyach, P. Thibault,
- 485 A Novel Differential Ion Mobility Device Expands the Depth of Proteome Coverage and the Sensitivity of
- 486 Multiplex Proteomic Measurements, *Mol Cell Proteomics* 17(10) (2018) 2051-2067.
- 487 [17] F. Meier, P.E. Geyer, S. Virreira Winter, J. Cox, M. Mann, BoxCar acquisition method enables single-
- 488 shot proteomics at a depth of 10,000 proteins in 100 minutes, *Nat Methods* 15(6) (2018) 440-448.
- 489 [18] F. Meier, A.D. Brunner, S. Koch, H. Koch, M. Lubeck, M. Krause, N. Goedecke, J. Decker, T. Kosinski,
- 490 M.A. Park, N. Bache, O. Hoerning, J. Cox, O. Rather, M. Mann, Online Parallel Accumulation-Serial
- 491 Fragmentation (PASEF) with a Novel Trapped Ion Mobility Mass Spectrometer, *Mol Cell Proteomics*
- 492 17(12) (2018) 2534-2545.
- 493 [19] J.N. Dodds, E.S. Baker, Ion Mobility Spectrometry: Fundamental Concepts, Instrumentation,
- 494 Applications, and the Road Ahead, *J Am Soc Mass Spectrom* 30(11) (2019) 2185-2195.
- 495 [20] F. Lanucara, S.W. Holman, C.J. Gray, C.E. Eyers, The power of ion mobility-mass spectrometry for
- 496 structural characterization and the study of conformational dynamics, *Nat Chem* 6(4) (2014) 281-94.
- 497 [21] V. Gabelica, A.A. Shvartsburg, C. Afonso, P. Barran, J.L.P. Benesch, C. Bleiholder, M.T. Bowers, A.
- 498 Bilbao, M.F. Bush, J.L. Campbell, I.D.G. Campuzano, T. Causon, B.H. Clowers, C.S. Creaser, E. De Pauw, J.
- 499 Far, F. Fernandez-Lima, J.C. Fjeldsted, K. Giles, M. Groessl, C.J. Hogan, Jr., S. Hann, H.I. Kim, R.T.
- 500 Kurulugama, J.C. May, J.A. McLean, K. Pagel, K. Richardson, M.E. Ridgeway, F. Rosu, F. Sobott, K.
- 501 Thalassinos, S.J. Valentine, T. Wyttenbach, Recommendations for reporting ion mobility Mass
- 502 Spectrometry measurements, *Mass Spectrom Rev* 38(3) (2019) 291-320.
- 503 [22] D.L. Tabb, L. Vega-Montoto, P.A. Rudnick, A.M. Variyath, A.J. Ham, D.M. Bunk, L.E. Kilpatrick, D.D.
- 504 Billheimer, R.K. Blackman, H.L. Cardasis, S.A. Carr, K.R. Clauser, J.D. Jaffe, K.A. Kowalski, T.A. Neubert,
- 505 F.E. Regnier, B. Schilling, T.J. Tegeler, M. Wang, P. Wang, J.R. Whiteaker, L.J. Zimmerman, S.J. Fisher,
- 506 B.W. Gibson, C.R. Kinsinger, M. Mesri, H. Rodriguez, S.E. Stein, P. Tempst, A.G. Paulovich, D.C. Liebler, C.
- 507 Spiegelman, Repeatability and reproducibility in proteomic identifications by liquid chromatography-
- 508 tandem mass spectrometry, *J Proteome Res* 9(2) (2010) 761-76.
- 509 [23] A.S. Hebert, S. Prasad, M.W. Belford, D.J. Bailey, G.C. McAlister, S.E. Abbatiello, R. Huguette, E.R.
- 510 Wouters, J.J. Dunyach, D.R. Brademan, M.S. Westphall, J.J. Coon, Comprehensive Single-Shot Proteomics
- 511 with FAIMS on a Hybrid Orbitrap Mass Spectrometer, *Anal Chem* 90(15) (2018) 9529-9537.
- 512 [24] S. Pfammatter, E. Bonneil, F.P. McManus, P. Thibault, Gas-Phase Enrichment of Multiply Charged
- 513 Peptide Ions by Differential Ion Mobility Extend the Comprehensiveness of SUMO Proteome Analyses, *J*
- 514 *Am Soc Mass Spectrom* 29(6) (2018) 1111-1124.
- 515 [25] C.D. Chouinard, G. Nagy, I.K. Webb, T. Shi, E.S. Baker, S.A. Prost, T. Liu, Y.M. Ibrahim, R.D. Smith,
- 516 Improved Sensitivity and Separations for Phosphopeptides using Online Liquid Chromatography Coupled
- 517 with Structures for Lossless Ion Manipulations Ion Mobility-Mass Spectrometry, *Anal Chem* 90(18)
- 518 (2018) 10889-10896.
- 519 [26] A.R. Ahmad Izaham, C.S. Ang, S. Nie, L.E. Bird, N.A. Williamson, N.E. Scott, What Are We Missing by
- 520 Using Hydrophilic Enrichment? Improving Bacterial Glycoproteome Coverage Using Total Proteome and
- 521 FAIMS Analyses, *J Proteome Res* 20(1) (2021) 599-612.
- 522 [27] K.E. Burnum-Johnson, S. Nie, C.P. Casey, M.E. Monroe, D.J. Orton, Y.M. Ibrahim, M.A. Gritsenko,
- 523 T.R. Clauss, A.K. Shukla, R.J. Moore, S.O. Purvine, T. Shi, W. Qian, T. Liu, E.S. Baker, R.D. Smith,
- 524 Simultaneous Proteomic Discovery and Targeted Monitoring using Liquid Chromatography, Ion Mobility
- 525 Spectrometry, and Mass Spectrometry, *Mol Cell Proteomics* 15(12) (2016) 3694-3705.

- 526 [28] B.M. Kolakowski, Z. Mester, Review of applications of high-field asymmetric waveform ion mobility
527 spectrometry (FAIMS) and differential mobility spectrometry (DMS), *Analyst* 132(9) (2007) 842-64.
- 528 [29] K.E. Swearingen, R.L. Moritz, High-field asymmetric waveform ion mobility spectrometry for mass
529 spectrometry-based proteomics, *Expert Rev Proteomics* 9(5) (2012) 505-17.
- 530 [30] S. Prasad, M.W. Belford, J.J. Dunyach, R.W. Purves, On an aerodynamic mechanism to enhance ion
531 transmission and sensitivity of FAIMS for nano-electrospray ionization-mass spectrometry, *J Am Soc*
532 *Mass Spectrom* 25(12) (2014) 2143-53.
- 533 [31] K.E. Swearingen, M.R. Hoopmann, R.S. Johnson, R.A. Saleem, J.D. Aitchison, R.L. Moritz, Nanospray
534 FAIMS fractionation provides significant increases in proteome coverage of unfractionated complex
535 protein digests, *Mol Cell Proteomics* 11(4) (2012) M111 014985.
- 536 [32] K.E. Swearingen, J.M. Winget, M.R. Hoopmann, U. Kusebauch, R.L. Moritz, Decreased Gap Width in
537 a Cylindrical High-Field Asymmetric Waveform Ion Mobility Spectrometry Device Improves Protein
538 Discovery, *Anal Chem* 87(24) (2015) 12230-7.
- 539 [33] D.H. Hock, B. Reljic, C.S. Ang, L. Muellner-Wong, H.S. Mountford, A.G. Compton, M.T. Ryan, D.R.
540 Thorburn, D.A. Stroud, HIGD2A is Required for Assembly of the COX3 Module of Human Mitochondrial
541 Complex IV, *Mol Cell Proteomics* 19(7) (2020) 1145-1160.
- 542 [34] L. Kall, J.D. Canterbury, J. Weston, W.S. Noble, M.J. MacCoss, Semi-supervised learning for peptide
543 identification from shotgun proteomics datasets, *Nat Methods* 4(11) (2007) 923-5.
- 544 [35] S. Tyanova, T. Temu, J. Cox, The MaxQuant computational platform for mass spectrometry-based
545 shotgun proteomics, *Nat Protoc* 11(12) (2016) 2301-2319.
- 546 [36] B. MacLean, D.M. Tomazela, N. Shulman, M. Chambers, G.L. Finney, B. Frewen, R. Kern, D.L. Tabb,
547 D.C. Liebler, M.J. MacCoss, Skyline: an open source document editor for creating and analyzing targeted
548 proteomics experiments, *Bioinformatics* 26(7) (2010) 966-8.
- 549 [37] S. Tyanova, T. Temu, P. Sinitcyn, A. Carlson, M.Y. Hein, T. Geiger, M. Mann, J. Cox, The Perseus
550 computational platform for comprehensive analysis of (prote)omics data, *Nat Methods* 13(9) (2016)
551 731-40.
- 552 [38] V.G. Tusher, R. Tibshirani, G. Chu, Significance analysis of microarrays applied to the ionizing
553 radiation response, *Proc Natl Acad Sci U S A* 98(9) (2001) 5116-21.
- 554 [39] D. Szklarczyk, A.L. Gable, D. Lyon, A. Junge, S. Wyder, J. Huerta-Cepas, M. Simonovic, N.T. Doncheva,
555 J.H. Morris, P. Bork, L.J. Jensen, C.V. Mering, STRING v11: protein-protein association networks with
556 increased coverage, supporting functional discovery in genome-wide experimental datasets, *Nucleic*
557 *Acids Res* 47(D1) (2019) D607-D613.
- 558 [40] B.K. Erickson, D.K. Schweppe, Q. Yu, R. Rad, W. Haas, G.C. McAlister, S.P. Gygi, Parallel Notched Gas-
559 Phase Enrichment for Improved Proteome Identification and Quantification with Fast Spectral
560 Acquisition Rates, *J Proteome Res* 19(7) (2020) 2750-2757.
- 561 [41] Q. Yu, J.A. Paulo, J. Naverrete-Perea, G.C. McAlister, J.D. Canterbury, D.J. Bailey, A.M. Robitaille, R.
562 Huguet, V. Zabrouskov, S.P. Gygi, D.K. Schweppe, Benchmarking the Orbitrap Tribrid Eclipse for Next
563 Generation Multiplexed Proteomics, *Anal Chem* 92(9) (2020) 6478-6485.
- 564 [42] D.B. Bekker-Jensen, A. Martinez-Val, S. Steigerwald, P. Ruther, K.L. Fort, T.N. Arrey, A. Harder, A.
565 Makarov, J.V. Olsen, A Compact Quadrupole-Orbitrap Mass Spectrometer with FAIMS Interface
566 Improves Proteome Coverage in Short LC Gradients, *Mol Cell Proteomics* 19(4) (2020) 716-729.
- 567 [43] Y. Cong, Y. Liang, K. Motamedchaboki, R. Huguet, T. Truong, R. Zhao, Y. Shen, D. Lopez-Ferrer, Y.
568 Zhu, R.T. Kelly, Improved Single-Cell Proteome Coverage Using Narrow-Bore Packed NanoLC Columns
569 and Ultrasensitive Mass Spectrometry, *Anal Chem* 92(3) (2020) 2665-2671.
- 570 [44] B. VanderSluis, M. Costanzo, M. Billmann, H.N. Ward, C.L. Myers, B.J. Andrews, C. Boone,
571 Integrating genetic and protein-protein interaction networks maps a functional wiring diagram of a cell,
572 *Curr Opin Microbiol* 45 (2018) 170-179.

- 573 [45] J. Han, K. Pluhackova, R.A. Bockmann, The Multifaceted Role of SNARE Proteins in Membrane
574 Fusion, *Front Physiol* 8 (2017) 5.
- 575 [46] W. Hong, S. Lev, Tethering the assembly of SNARE complexes, *Trends Cell Biol* 24(1) (2014) 35-43.
- 576 [47] J. Malsam, T.H. Sollner, Organization of SNAREs within the Golgi stack, *Cold Spring Harb Perspect*
577 *Biol* 3(10) (2011) a005249.
- 578 [48] O. Laufman, W. Hong, S. Lev, The COG complex interacts directly with Syntaxin 6 and positively
579 regulates endosome-to-TGN retrograde transport, *J Cell Biol* 194(3) (2011) 459-72.
- 580

581



582

583

584 **Figure 1.** A 3X FLAG tag specific Co-IP Mass spectrometry experiment on an Orbitrap Fusion Lumos mass

585 spectrometer. (A) The TIC mass spectrum showing the the most intense peaks between 18-22minutes. (B)

586 The averaged mass spectrum at ~19min showing the presence of the oxidized version of the 3X FLAG

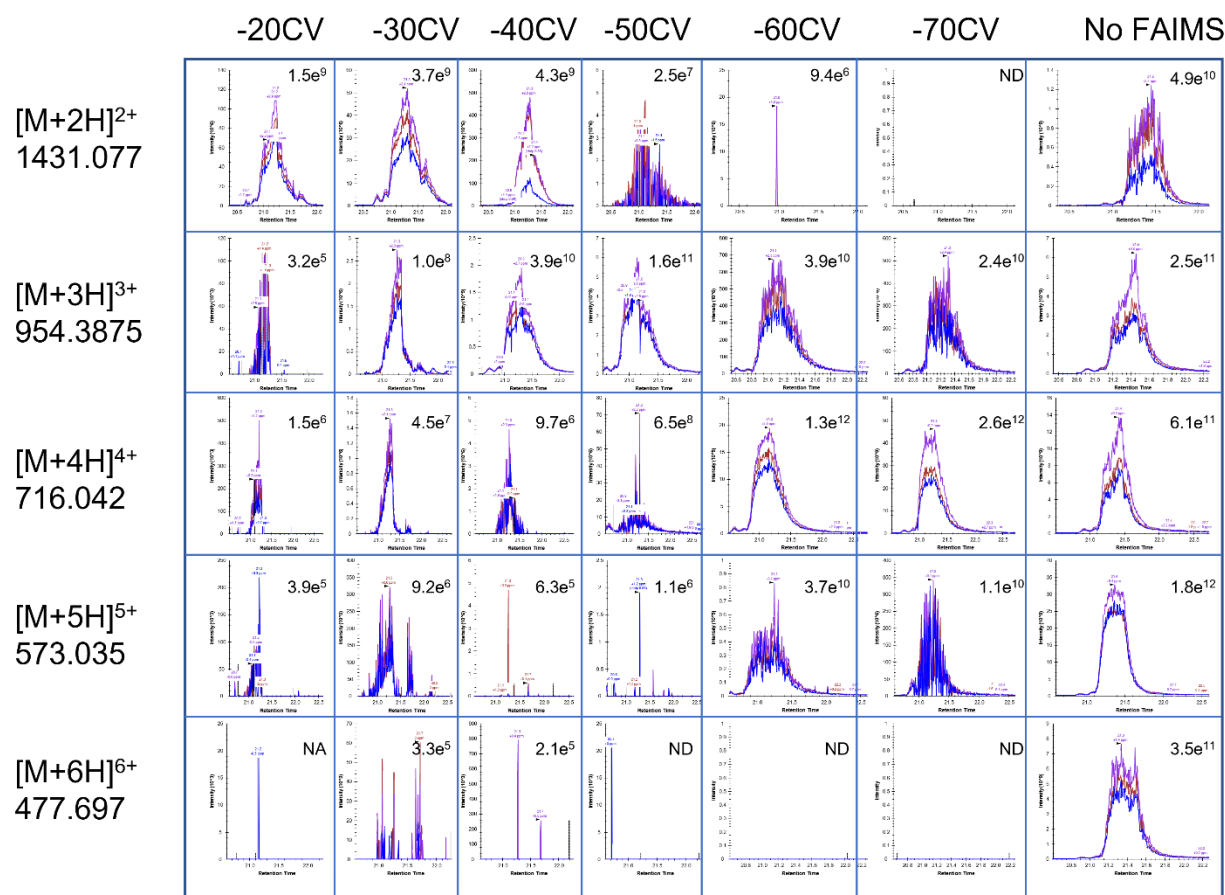
587 peptide and a trypsin derived truncated version of the 3X FLAG peptide. (C) The averaged mass spectrum

588 at ~21min showing the charge distribution of the intact 3X FLAG peptide. Note m/z peak labeling is on the

589 most abundant ion in the isotopic cluster.

590

591



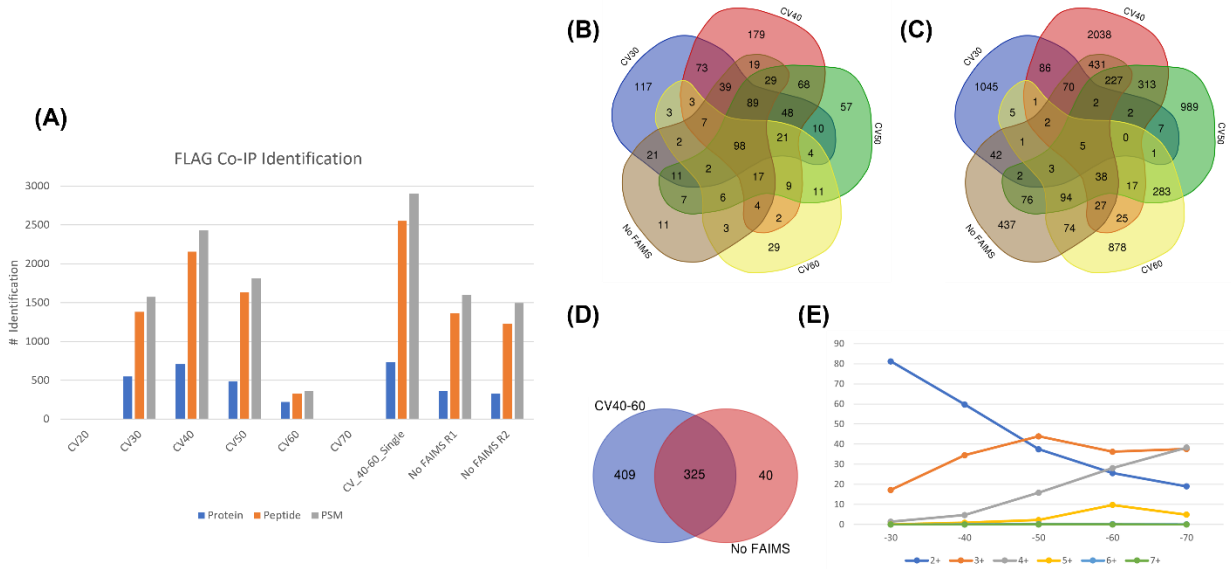
592

593

594 Figure 2: Monitoring the intensities of the different charge species of the 3X FLAG peptide across the

595 different CVs. The extracted ion chromatogram of all graphs is centered at 21.3 min and inserts values

596 represent the total area information. ND = not detected. Metadata is available in Supplementary Table 1.



597

598

599 **Figure 3.** Analyzing the protein and peptide identification from the FLAG Co-IP experiment. (A) Breakdown

600 of protein, peptide and PSM across 6 different CVs, two internal CV stepping and two replicates without

601 FAIMS. We did not identify any proteins with CV-20 and CV-70. (B) Venn diagram of unique protein

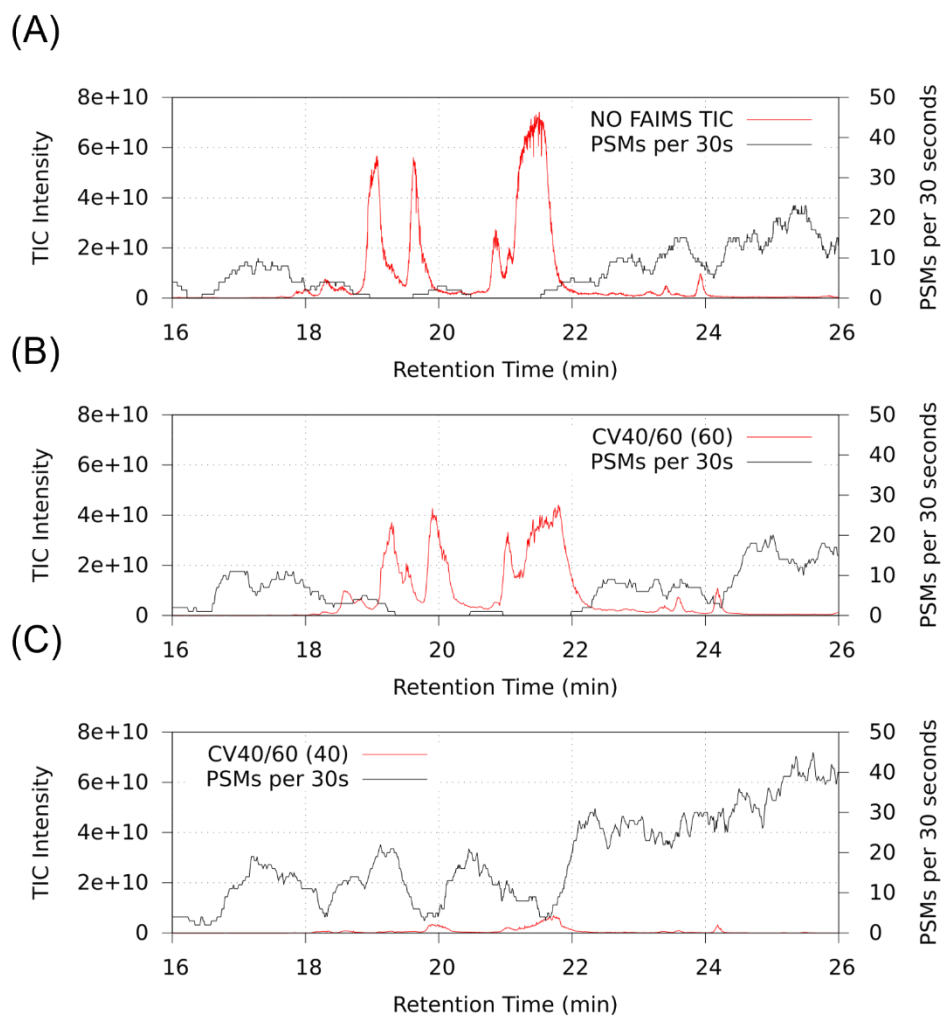
602 identification across 4 different CVs (-30, -40, -50 and -60) with No FAIMS applied. (C) Venn diagram of

603 unique peptide identification across 4 different CVs (-30, -40, -50 and -60) with No FAIMS applied. (D)

604 Proteins that are uniquely identified with 2 internal CV stepping vs without FAIMS (E) Charge distribution

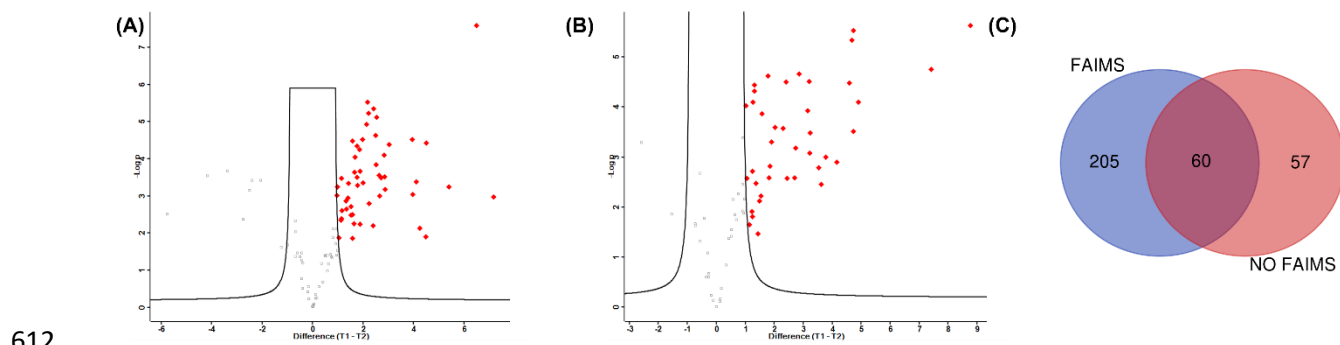
605 of MS1 precursors selected for MSMS across the 6 different CVs.

606

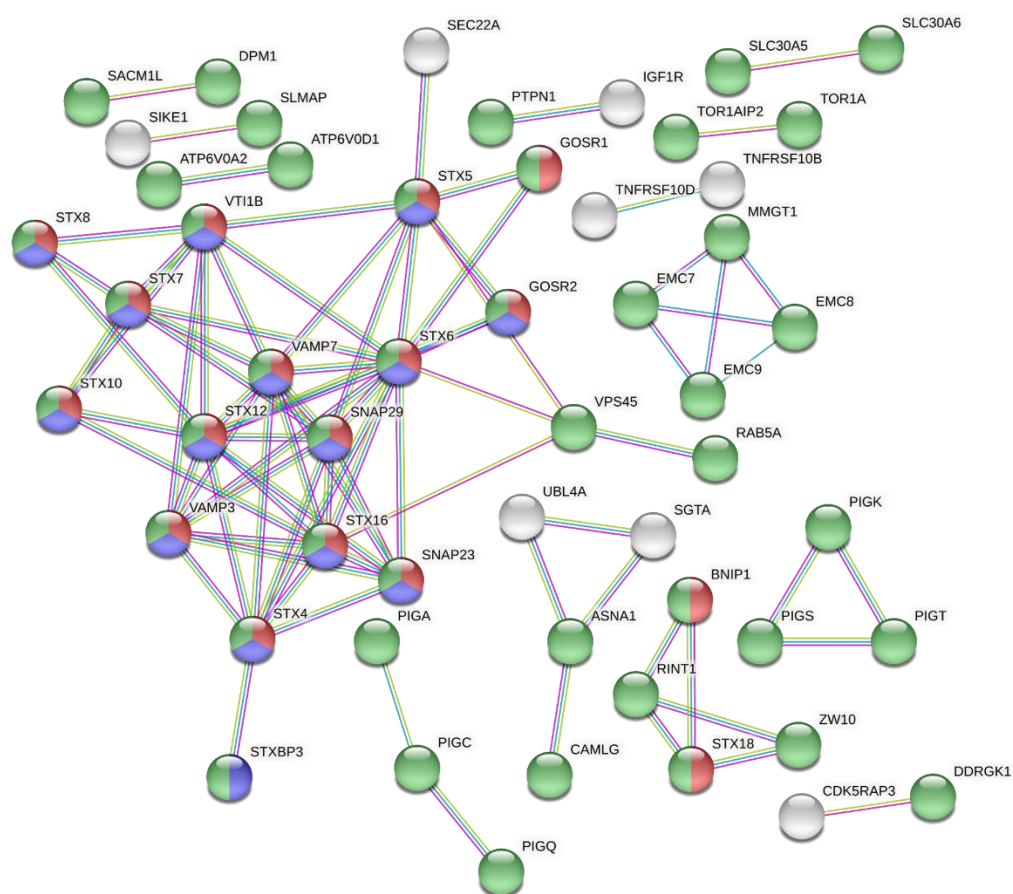


607

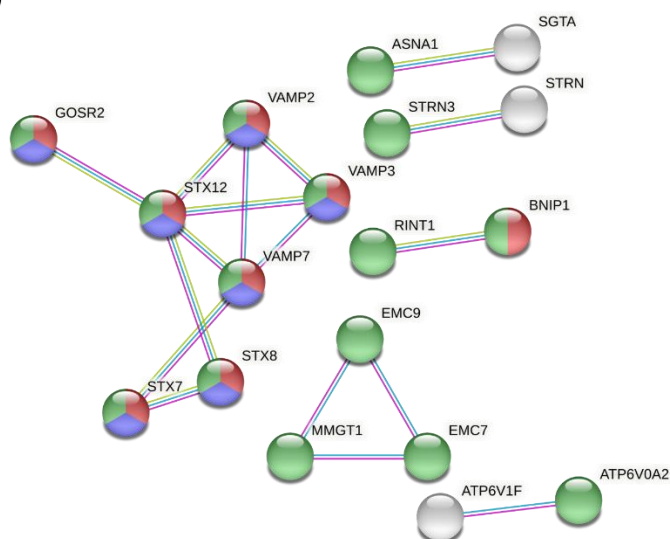
608 Figure 4: Plot of total ion chromatogram (red trace) and PSM identification (black trace) from the FLAG-
609 Tag Co-IP experiment with (switching between CVs of -40 and -60) and without FAIMS at retention time
610 16 to 26 min. (A) Experiment without FAIMS (B) Extracted TIC and PSM with FAIMS at CV-60 (C) Extracted
611 TIC and PSM with FAIMS at CV-40.



(D)



(E)



614

615 Figure 5: Protein-protein interaction from Co-IP with and without FAIMS (A) Volcano plot from the FAIMS
616 enabled experiment and highlighting proteins (red diamond) that have significantly increased in
617 abundances in drug treated samples (proteins identified in 3 replicates, T-Test, FDR 0.05 and $S_0=2$). X-axis
618 represents \log_2 transformed fold change and y-axis represents the T-test p values. (B) Volcano plot from
619 the without FAIMS experiment and highlighting proteins (red diamond) that have significantly increased
620 in abundances in drug treated samples (C) Venn diagram of proteins submitted to STRING analysis. These
621 include proteins significantly increased and proteins exclusively found in the drug treatment groups
622 (identified in all 3 replicates of the drug treated group and absent in the other group). (D) STRING physical
623 subnetwork analysis for the FAIMS enabled experiment. For clarity, disconnected nodes have been
624 hidden. Red and blue bubble represent molecular functions enriched in SNAP receptor (p-value = 5.14e-
625 16) and SNARE binding activity (p-value = 3.56e-08), respectively. Green bubble represents enrichment in
626 the endomembrane system (p-value = 1.53e-61). (E) STRING physical subnetwork analysis for without
627 FAIMS experiment. For clarity, discontinued nodes have been hidden. Red and blue bubble represent
628 molecular functions enriched in SNAP receptor (p-value = 2.11e-08) and SNARE binding activity,
629 respectively (p-value = 0.0015), respectively. Green bubble represents enrichment in the endomembrane
630 system (p-value = 1.73e-31). Edges color legend: Pink = experimentally defined, Magenta = from curated
631 databases and Light Green = text mining

632